Journal of Naval Sciences and Engineering
2023, Vol. 19, No. 1, pp. 53-76 *DOI: 10.56850/jnse.1250094*
Shipbuilding and Ocean Engineering/Gemi ve Deniz Teknolojisi Mühendisliği

RESEARCH ARTICLE

**An ethical committee approval and/or legal/special permission has not been required within the scope of this study.*

SCALE EFFECTS ON THE LINEAR HYDRODYNAMIC COEFFICIENTS OF DARPA SUBOFF*

Furkan KIYÇAK[1]
Ömer Kemal KINACI[2]

[1]*Istanbul Technical University, Department of Shipbuilding & Ocean Engineering, Istanbul, Turkey,*
kiycak15@itu.edu.tr

[2]*Istanbul Technical University, Department of Shipbuilding & Ocean Engineering, Istanbul, Turkey,*
kinacio@itu.edu.tr

Received: 11.02.2023 **Accepted: 15.03.2023**

ABSTRACT

It is well known that forces and moments acting on a ship are functions of Froude and Reynolds numbers. As a ship gets larger in size, these two numbers grow, which leads to different flow regimes around the hull. However, the state-of-the-art in maneuvering calculations is to consider the hydrodynamic coefficients as constants for model and full ship scales. For submerged bodies, the Froude number is insignificant due to the distant free water surface; therefore, these forces only depend on the Reynolds number. In this study, we consider the benchmark 'DARPA' Suboff form, which is extensively studied in the literature, and investigated the scale effects on the hydrodynamic coefficients with respect to the Reynolds number. Numerical studies are carried out on the bare hull form of the submarine. Captive motions of static drift and pure yaw motions are conducted utilizing the oblique towing and rotating arm tests via RANS-based CFD. Linear hydrodynamic coefficients are expressed with logarithmic equations as functions of the Reynolds number, explicitly showing the dependency on the ship's model scale.

Keywords: *CFD, DARPA, maneuvering derivatives, pure yaw, static drift.*

Scale Effect on The Linear Hydrodynamic Coefficients of DARPA Suboff

LİNEER HİDRODİNAMİK KATSAYILARIN HESABINDA ÖLÇEK ETKİSİ

ÖZ

Gemiye etki eden kuvvetlerin ve momentlerin Froude ve Reynolds sayılarının fonksiyonları oldukları iyi bilinmektedir. Geminin boyutu büyüdükçe, bu iki sayı da büyür ve bu da gövde etrafında farklı akış rejimlerine yol açar. Bununla birlikte, manevra hesaplamalarında, hidrodinamik katsayılar, model ve tam gemi ölçekleri için sabit olarak kabul edilmektedir. Suya batık cisimler için, uzaktaki serbest su yüzeyi nedeniyle Froude sayısı önemsizdir; bu nedenle, bu kuvvetler yalnızca Reynolds sayısına bağlıdır. Bu çalışmada, literatürde yoğun olarak çalışılan ve bir referans noktası niteliğindeki 'DARPA' Suboff formunu ele aldık ve ölçeğin hidrodinamik katsayılar üzerindeki etkilerini Reynolds sayısına göre inceledik. Denizaltının çıplak gövde formu üzerinde sayısal çalışmalar yapılmış, RANS tabanlı CFD aracılığıyla çekme tankı ve dönen kol testleri kullanılarak statik sürüklenme ve safi savrulma hareketleri gerçekleştirilmiştir. Lineer hidrodinamik katsayılar, Reynolds sayısının fonksiyonları olarak logaritmik denklemlerle ifade edilmiş ve geminin model ölçeğine bağımlılığı açıkça gösterilmiştir.

Anahtar Kelimeler: *DARPA, HAD, manevra türevleri, safi savrulma, statik sürüklenme.*

1. INTRODUCTION

As a result of developing technology and increasing computer capacities, the precision and importance of computational analysis are increasing day by day. In naval architecture, the ship hydrodynamics field has been positively affected by these developments due to the intense mathematical and physical computations involved.

Several different methods can be used in assessing the hydrodynamic performance of ships. These are empirical methods, model experiments, and computational fluid dynamics methods (Can, 2014). It is the navies that typically place submarines at the center of their attention, and, due to this reason, any research related to them is kept confidential. Although there are numerous empirical relations available for use, hydrodynamic analysis based on these formulas is not adequate and reliable. Model experiments are very useful but are both expensive and time-consuming (Budak & Beji, 2016). The last method, computational fluid dynamics, or CFD, has become very popular in recent years and its use is becoming widespread. With the advancement of modern CFD techniques, the method is believed to give pretty accurate estimates (He et al., 2016). Not only is it less expensive than conducting model experiments, CFD allows analyzing higher Reynolds number flows, making it a better alternative to empirical formulas.

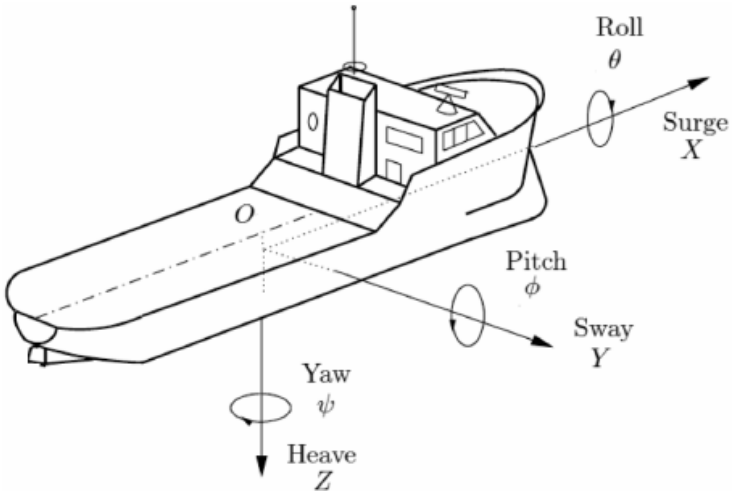

Figure 1. 6 DOF for ship motions (Krishna Kumar et al., 2018).

Ships, like any other mechanical body, possess six degrees-of-freedom (6DOF), as illustrated in Figure 1. Roll, pitch, and heave are defined in the vertical plane and mostly investigated in seakeeping. Surge, sway, and yaw are defined as horizontal plane motions and generally studied in maneuvering. Maneuverability is closely related to navigational safety and accurate calculation prior to the construction state is crucial. Briefly, maneuverability is the ability of a ship to change direction in a controlled manner in desired direction and continue without deviating from its route after this change (Sukas et al., 2017).

Today, navigation safety is a design parameter of greater significance in navy projects compared to commercial ones. When it comes to the design process, submarines vary significantly from surface ships in navy projects, with distinct design properties and concepts. Recent heavy investments in the defense industries from developed and developing countries increased the importance of studies based on submarines. Scientific studies on underwater hydrodynamics have gained momentum recently. For instance, the approaches used to evaluate the maneuvering capability of underwater vehicles are examined by Kirikbas et al. (2021). Linear and nonlinear hydrodynamic coefficients of underwater vehicles are evaluated using CFD by Ray et al. (2009). The scale effect on horizontal maneuvering derivatives of an underwater vehicle is investigated by Kahramanoglu (2023). Maneuvering of an underwater vehicle is simulated using CFD based method by Racine & Paterson (2005). Maneuvering forces on submarines using two viscous-flow solvers are calculated by Vaz et al. (2010). In addition, an experimental study was carried out in which linear hydrodynamic coefficients were calculated by Roddy (1990). That study provides the opportunity to compare the EFD results with the numerical studies of the DARPA form in deep water that has been studied in detail.

The governing Navier-Stokes equations for fluid flows implicate several non-dimensional parameters (namely Strouhal, Weber, Euler, Reynolds, and Froude numbers) to be acting on bodies in fluids. Not all of these parameters have significant effect on ships: the force and moment acting on a ship are functions of the Froude and Reynolds numbers and generally expressed in terms of these numbers. Hydrodynamic derivatives should be calculated to specify the maneuvering performance both on the water

surface or in deep water (Cavdar & Bal, 2022). Different from surface ships (because there are no waves far from the water surface), hydrodynamic forces will be independent from the Froude number for submarines. Therefore, in this paper, only the effects of the Reynolds number on maneuvering derivatives are investigated to assess the scale effect on a ship's maneuvering performance. The ship discussed in our study is the 'DARPA' submarine bare hull form, which is widely used in the literature.

In this paper, numerical analyses of static drift mentioned as oblique towing test, and pure yaw mentioned as rotating arm test in the literature are investigated with the help of CFD. Since the effect of the Reynolds number on the maneuvering derivatives of the DARPA Suboff is to be examined, the static drift and pure yaw analyses were completed at various sizes and speeds (which also changes the Reynolds numbers). From the CFD simulations, the forces and moments acting on the ship are obtained. These are graphed with respect to the ship's sway velocity v and yaw rate r. Then, equations are generated using a curve-fitting tool. These equations return Y_v, Y_r, N_v, and N_r for each studied case. Then, these linear hydrodynamic coefficients are graphed with respect to the Reynolds number. Results are generalized with logarithmic equations and a correlation was obtained between the maneuvering derivatives and the Reynolds number.

2. GEOMETRY AND MATHEMATICAL MODEL

2.1. Geometry

The properties of the bare hull form of the DARPA geometry named AFF-1 configuration at the scale that the model experiments done are shown in Table 1. The three-dimensional model of the form is shown in Figure 2.

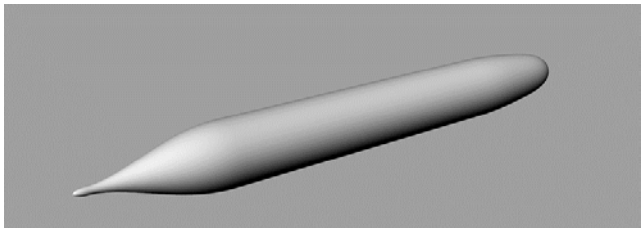

Figure 2. DARPA bare hull 3-D model.

Table 1. DARPA bare hull form properties.

Parameter	Value
Length Between Perpendiculars (m)	4.261
Length Overall (m)	4.356
Length of Forebody (m)	1.016
Length of Parallel Middlebody (m)	2.229
Length of Run (m)	1.111
Diameter (m)	0.508
LCB (m)	2.008
x_G (m)	0.0092

2.2. Equations of Motion

As mentioned in the introduction, when maneuverability is examined, usually a 3 DOF axis set is used (Sukas et al., 2019). These are surge representing translation in the x-axis, sway representing translation in the y-axis, and yaw representing rotation around the z-axis. The force calculated from the surge motion represents the resistance and is studied within the resistance problems. According to Newton's second law, Earth-fixed force and moment can be identified in the general form in equations 1, 2, and 3:

$$X_0 = m\ddot{x}_G \tag{1}$$

$$Y_0 = m\ddot{y}_G \tag{2}$$

$$N = I_Z\dot{r} \tag{3}$$

In maneuvering, the sway and yaw effects are more dominant when compared with the surge. Therefore, it is possible to implement 2 DOF ship motion equations, which can be expressed as below:

$$(m + m_y)\dot{v} + (m + m_x)ur + x_G m\dot{r} = Y \tag{4}$$

$$(I_{zG} + {x_G}^2 m + J_z)\dot{r} + x_G m(\dot{v} + ur) = N \tag{5}$$

In equations 4 and 5, the right-hand side consists of the hull, the propeller, and the rudder for a conventional ship. We only focus on the linear hydrodynamic coefficients of the hull in this paper; therefore, linear terms can be identified as $Y_{\dot{v}}$, Y_v, $Y_{\dot{r}}$, Y_r, $N_{\dot{v}}$, N_v, $N_{\dot{r}}$, and N_r. Four of these terms are based on the added mass, which is extensively studied in the literature before. In this respect, we only paid attention to Y_v, Y_r, N_v, and N_r. After obtaining the forces and moments acting on the ship via CFD, they are nondimensionalized as in Table 2: (Feldman J, 1979)

Table 2. Nondimensionalization.

Parameter	Nondimensionalization	Notation
v	v/U	v'
X	$X/0.5*\rho*U^2*L_{pp}^2$	X'
Y	$Y/0.5*\rho*U^2*L_{pp}^2$	Y'
N	$N/0.5*\rho*U^2*L_{pp}^3$	N'

Since the studied geometry is bare hull form, hydrodynamic force and moment on the hull can be expressed with 2 DOF as in equations 6 and 7: (Yasukawa & Yoshimura, 2015)

$$Y'_H = Y'_v v' + (Y'_r - m' - m'_x)r' + Y'_{vvv}v'^3 + Y'_{vvr}v'^2 r' + Y'_{vrr}v' r'^2 + Y'_{rrr}r'^3 \quad (6)$$

$$N'_H = N'_v v' + (N'_r - m' x'_G)r' + N'_{vvv}v'^3 + N'_{vvr}v'^2 r' + N'_{vrr}v' r'^2 + N'_{rrr}r'^3 \quad (7)$$

In these equations, $Y'_v, Y'_{vvv}, N'_v,$ and N'_{vvv} maneuvering derivatives are obtained from the static drift analysis results, $Y'_r, Y'_{rrr}, N'_r,$ and N'_{rrr} maneuvering derivatives are obtained from the pure yaw analysis results with the multiple run method (Yoon, 2009). Other maneuvering derivatives are not investigated in this article.

3. NUMERICAL MODEL AND COMPUTATIONAL METHOD

Hydrodynamic forces and moments are solved with the commercial RANS solver program ANSYS Fluent by finite volume method (FVM) with the discretization of continuity and Navier-Stokes equations. The 'SIMPLE' algorithm is used in both static drift and pure yaw and a second-order

solution was made for pressure, momentum, and turbulence. SST k-ω was chosen as the turbulence model. While creating the boundary layer, y^+=30 is assumed. In all analyses, the density of seawater is taken at 997.51 kg/m^3, and the kinematic viscosity of seawater is taken at 10^{-6} m^2/s.

3.1. Static Drift

In static drift, the object in the fluid is towed at different drift angles and the sway force and the yaw moment are measured. In the static drift study, the mesh was created with the Pointwise, which is the mesh generation program for CFD. In all cases, when creating the fluid domain, a distance of about 1.5L from the front of the object, about 2.5L from the back, and about 2L left in the other directions. Examples of mesh views of static drift are shown in Figure 3.

Table 3. Static drift cases.

Parameter	**Case 1**	**Case 2**	**Case 3**	**Case 4**	**Case 5**	**Case 6**
L_{pp} (m)	4.261	2.130	8.522	4.261	2.130	8.522
U_0 (m/s)	1.50	1.50	1.50	2.50	2.50	2.50
Re	6.36E+06	3.18E+06	1.27E+07	1.06E+07	5.30E+06	2.12E+07
Parameter	**Case 7**	**Case 8**	**Case 9**	**Case 10**	**Case 11**	**Case 12**
L_{pp} (m)	4.261	2.130	8.522	1.065	2.130	2.130
U_0 (m/s)	4.00	4.00	4.00	1.00	0.25	0.75
Re	1.70E+07	8.48E+06	3.39E+07	1.06E+06	5.30E+05	1.59E+06

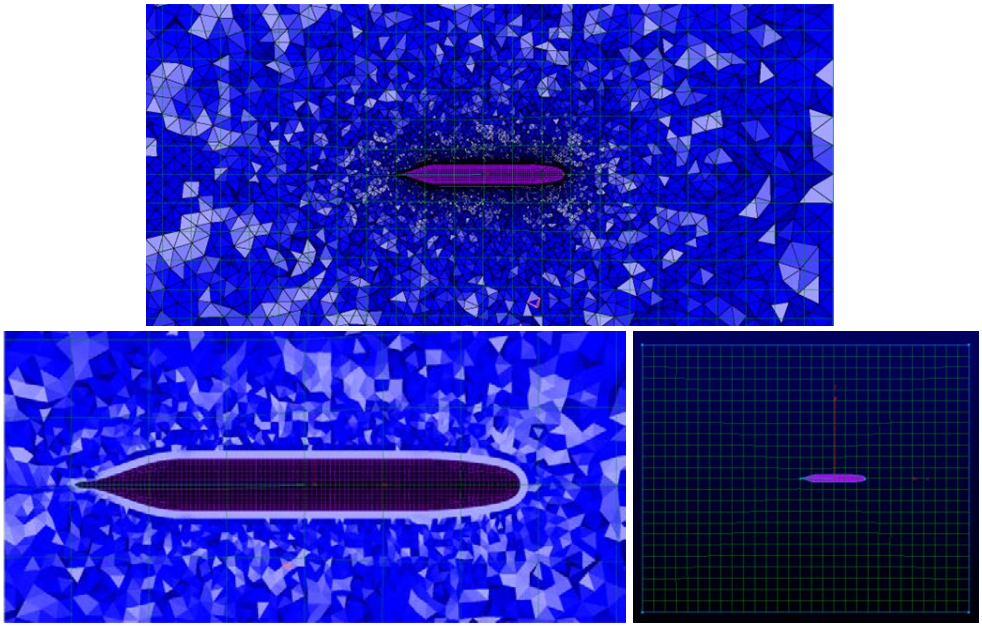

Figure 3. Example of static drift mesh views.

Static drift analysis was carried out at 12 different Reynolds numbers by scaling the length and service speed of the submarine. These 12 different cases are shown in Table 3.

In each of these 12 different situations, the flow was sent on the submarine at a drift angle of 0º, 3º, 6º, 9º, 12º, and 15º, and sway force Y and yaw moment N were taken as outputs. The values for Case 1 are given in Table 4.

Table 4. Forces and moments for Case 1.

β (deg)	β (rad)	v (m/s)	Y (N)	N (Nm)
0	0	0	0	0
3	0.0524	-0.0785	7.616	61.923
6	0.1047	-0.1568	18.567	119.504
9	0.1571	-0.2347	36.445	168.915
12	0.2094	-0.3119	64.011	208.230
15	0.2618	-0.3882	101.270	240.418

The lateral velocity is given in Table 4 and can be calculated with the help of the $v = U_0 * \sin\beta$ relation where β is drift angle, v is lateral velocity and U_0 is service speed.
Then, velocity, force and moment values are made nondimensional. Non-dimensional values for Case 1 are shown in Table 5.

Table 5. Nondimensional forces and moments for Case 1.

v'	**Y'**	**N'**
0	0	0
-0.0523	0.00037	0.00071
-0.1045	0.00091	0.00138
-0.1564	0.00179	0.00195
-0.2079	0.00314	0.00240
-0.2588	0.00497	0.00277

Thereafter, with help of the mathematical models given in equations 8 and 9, fitted the optimal curve based on the models (Shenoi et al., 2013). With the help of the obtained force and moment values and mathematical model, linear hydrodynamic coefficients Y_v and N_v were obtained (Triantafyllou & Hover, 2003). Coefficients given in the Results part.

$$Y' = Y_v{}'v' + Y_{vvv}{}'v'^3 \quad (8)$$

$$N' = N_v{}'v' + N_{vvv}{}'v'^3 \quad (9)$$

Y_{vvv} and N_{vvv} are nonlinear derivatives of maneuvering and were not analyzed in this study.

3.2. Pure Yaw

In pure yaw, the submarine rotates around a fixed arm length of R with a constant speed of r. In the pure yaw study, the mesh was created within the commercial ANSYS program. Since the length of the arm of rotation changed in each of the 12 different situations, the distances left while creating the fluid domain could not be standardized, but care was taken to leave such a distance not to disturb the flow around the object. Examples of mesh views of pure yaw are shown in Figure 4.

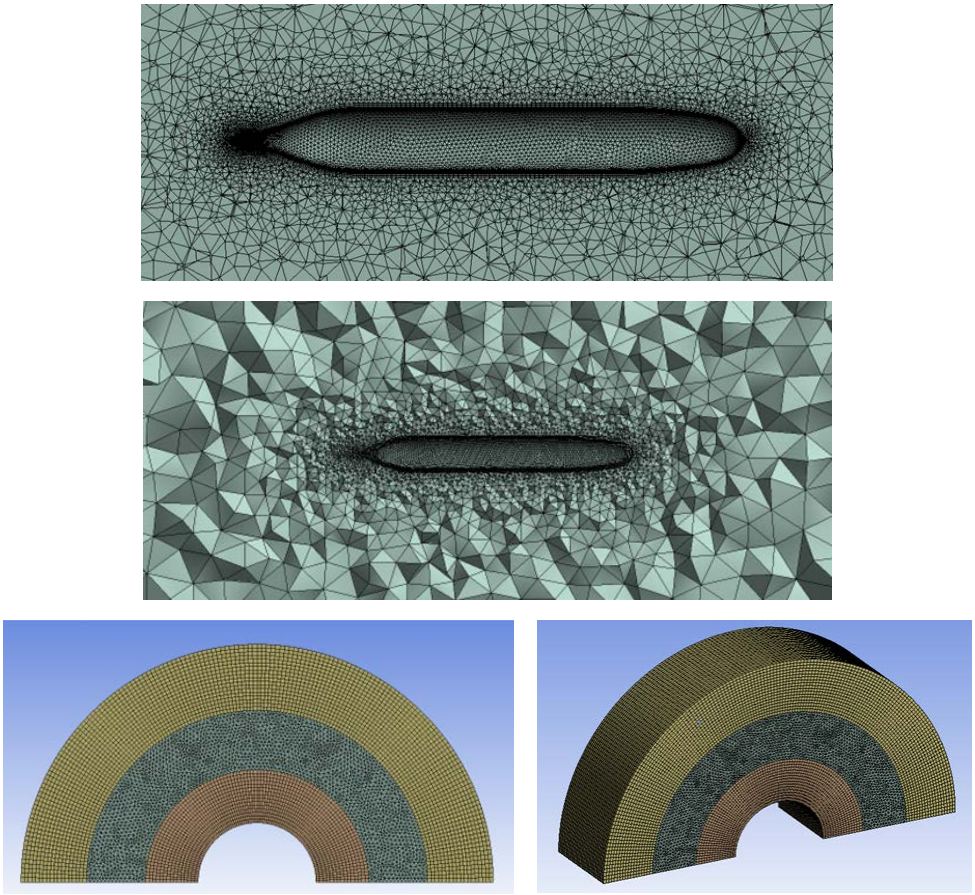

Figure 4. Example of pure yaw mesh views.

Pure yaw analysis was carried out at 12 different Reynolds numbers by scaling the length and service speed of the submarine. These 12 different cases are shown in Table 6.

In these 12 cases, the r'max values were taken as 0.1, 0.2, 0.4, 0.6, and 0.8, the rotational speeds were calculated with r'max = rL/U_0 relation, and the rotation arm length was found with the help of the $U_0 = rR$. As a result of the analyses, sway force Y and yaw moment N are taken as outputs. The values for Case 1 are given in Table 7. Then, velocity, force, and moment values are made nondimensional. Non dimensional values for Case 1 are shown in Table 8.

Table 6. Pure yaw cases.

Parameter	**Case 1**	**Case 2**	**Case 3**	**Case 4**	**Case 5**	**Case 6**
L_{pp} (m)	4.261	2.130	8.522	4.261	2.130	8.522
U_0 (m/s)	1.50	1.50	1.50	2.50	2.50	2.50
Re	6.36E+06	3.18E+06	1.27E+07	1.06E+07	5.30E+06	2.12E+07
Parameter	**Case 7**	**Case 8**	**Case 9**	**Case 10**	**Case 11**	**Case 12**
L_{pp} (m)	4.261	2.130	8.522	1.065	2.130	2.130
U_0 (m/s)	4.00	4.00	4.00	1.00	0.25	0.75
Re	1.70E+07	8.48E+06	3.39E+07	1.06E+06	5.30E+05	1.59E+06

Table 7. Forces and moments for Case 1.

r' (rad)	**r (rad/s)**	**R (m)**	**Y (N)**	**N (Nm)**
0.1	0.0352	42.609	1.584	-8.824
0.2	0.0704	21.305	3.448	-18.421
0.4	0.1408	10.652	9.017	-40.624
0.6	0.2112	7.102	15.734	-65.423
0.8	0.2816	5.326	24.895	-96.693

Table 8. Nondimensional forces and moments for Case 1.

r'	**Y'**	**N'**
0.1	0.00008	-0.00010
0.2	0.00017	-0.00021
0.4	0.00044	-0.00047
0.6	0.00077	-0.00075
0.8	0.00122	-0.00111

Thereafter, with help of the mathematical models given in equations 10 and 11, fitted the optimal curve based on the models (Rajita Shenoi et al., 2013). With the help of the obtained force and moment values and mathematical

model, linear hydrodynamic coefficients Y_r and N_r were obtained (Triantafyllou & Hover, 2003). Coefficients given in the Results part.

$$Y' = Y_r{}'r'_{max} + Y_{rrr}{}'r'^{3}_{max} \quad (10)$$

$$N' = N_r{}'r'_{max} + N_{rrr}{}'r'^{3}_{max} \quad (11)$$

Y_{rrr} and N_{rrr} are nonlinear derivatives of maneuvering and were not analyzed in this study.

4. GRID INDEPENDENCY

As a key factor in CFD, grid resolution is one of the most important elements for user decision making. Today, most scientific studies and simulations require grid-independent CFD solutions as a first and basic rule. A grid-independent CFD solution is achieved when the difference between numerical solutions at different grid numbers is negligible. The choice of grids to be tested and the determination of the grid-independent solution are at the discretion of the CFD user (Wang & Zhai, 2012).

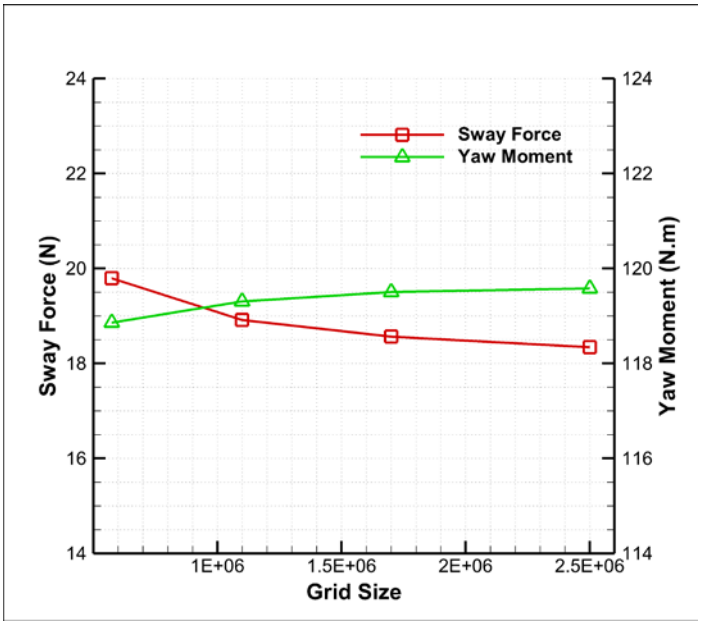

Figure 5. Grid convergence.

The grid convergence study was performed by developing four different meshes: with coarse, medium, medium-fine, and fine grids for 6 degrees static drift simulation in Case 1. The cell numbers varied from $5.75*10^5$ to $2.50*10^6$ for illustrating the sway force and yaw moment convergence as shown in Table 9 and Figure 5. It was found that there was no significant change in sway force (Y) and yaw moment (N) beyond the "medium-fine" grid density. Therefore, for the present paper, "medium-fine" grid density was used to perform all the simulations.

Table 9. Comparison of Y and N for different grid sizes.

Grid	Elements	Y (N)	N (N.m)
Coarse	575000	19.792	118.861
Medium	1100000	18.915	119.308
Medium-Fine	1700000	18.567	119.504
Fine	2500000	18.342	119.579

5. RESULTS

Static drift and pure yaw analyses were performed at 12 different Reynolds numbers. Static drift was completed at 0º, 3º, 6º, 9º, 12º ve 15º drift angles in each of these 12 cases, and pure yaw was completed for r'max values 0.1, 0.2, 0.4, 0.6, and 0.8 in each of the 12 cases.

Table 10. Linear hydrodynamic coefficients of static drift.

	L_{pp}	U_0	Re	Y_v'	N_v'
Case 1	4.261	1.50	6.36E+06	-0.006930	-0.013508
Case 2	2.130	1.50	3.18E+06	-0.008198	-0.013187
Case 3	8.522	1.50	1.27E+07	-0.006306	-0.013691
Case 4	4.261	2.50	1.06E+07	-0.006504	-0.013615
Case 5	2.130	2.50	5.30E+06	-0.007829	-0.013385
Case 6	8.522	2.50	2.12E+07	-0.005964	-0.013798
Case 7	4.261	4.00	1.70E+07	-0.006217	-0.013720

Case 8	2.130	4.00	8.48E+06	-0.007335	-0.013552
Case 9	8.522	4.00	3.39E+07	-0.005768	-0.013927
Case 10	1.065	1.00	1.06E+06	-0.011218	-0.012429
Case 11	2.130	0.25	5.30E+05	-0.011604	-0.012380
Case 12	2.130	0.75	1.59E+06	-0.009394	-0.012737
EFD	4.261	3.34	1.42E+07	-0.005948	-0.012795

5.1. Static Drift

After calculating Y_v' and N_v' in each Reynolds number, the distribution graph of hydrodynamic coefficients according to the Reynolds number was drawn and the most appropriate equation was selected. The calculated maneuvering derivatives and the experimental results published by DTRC (Roddy, 1990) are shown in Table 10, and the graphics are shown in Figure 6 and Figure 7.

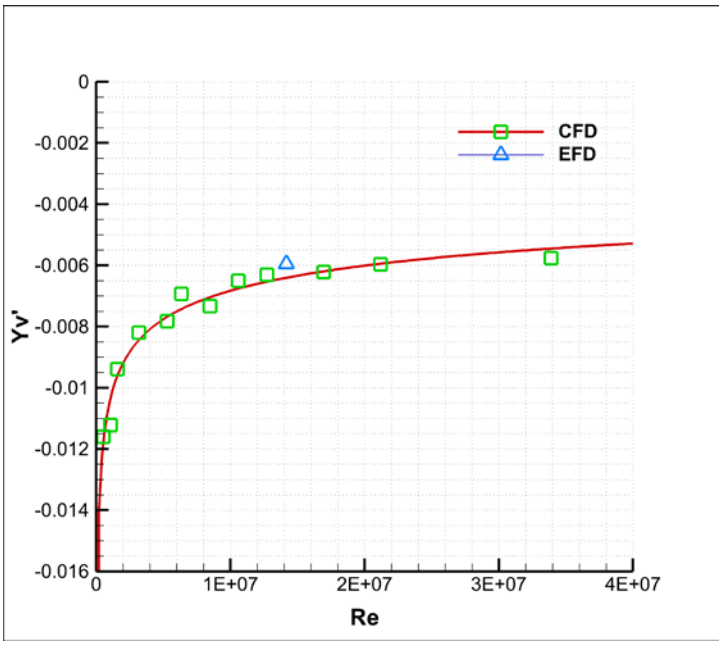

Figure 6. Re-Y_v' distribution of static drift.

Equation 12 and Equation 13 were obtained when the collected data as a result of CFD were fitted to the most appropriate equations. So, based on these two equations, if we have the Reynolds number of the bare hull form of the DARPA, we can calculate the Y_v' and N_v'.

$$Y_v' = 0.001527353 \ln(\mathrm{Re}) - 0.03154784 \quad (12)$$

$$N_v' = -0.000410797 \ln(\mathrm{Re}) - 0.006932722 \quad (13)$$

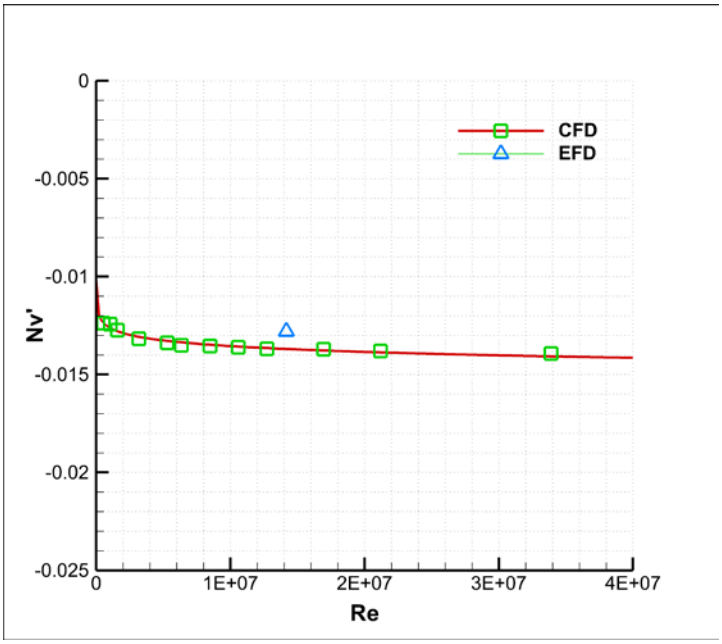

Figure 7. Re-N_v' distribution of static drift.

Table 11. Linear hydrodynamic coefficients of pure yaw.

	L_{pp}	U_0	Re	Y_r'	N_r'
Case 1	4.261	1.50	6.36E+06	0.001832	-0.001076
Case 2	2.130	1.50	3.18E+06	0.002116	-0.001225
Case 3	8.522	1.50	1.27E+07	0.001733	-0.001014
Case 4	4.261	2.50	1.06E+07	0.001749	-0.001021
Case 5	2.130	2.50	5.30E+06	0.001881	-0.001100
Case 6	8.522	2.50	2.12E+07	0.001691	-0.000980

Case 7	4.261	4.00	1.70E+07	0.001698	-0.000983
Case 8	2.130	4.00	8.48E+06	0.001780	-0.001027
Case 9	8.522	4.00	3.39E+07	0.001656	-0.000959
Case 10	1.065	1.00	1.06E+06	0.002467	-0.001469
Case 11	2.130	0.25	5.30E+05	0.002031	-0.001396
Case 12	2.130	0.75	1.59E+06	0.002486	-0.001435
EFD	4.261	3.34	1.42E+07	0.001811	-0.001597

5.2. Pure Yaw

After calculating Y_r' and N_r' in each Reynolds number, the distribution graph of hydrodynamic coefficients according to the Reynolds number was drawn and the most appropriate equation was selected. The calculated maneuvering derivatives and the experimental results published by DTRC (Roddy, 1990) are shown in Table 11, and the graphics are shown in Figure 8 and Figure 9.

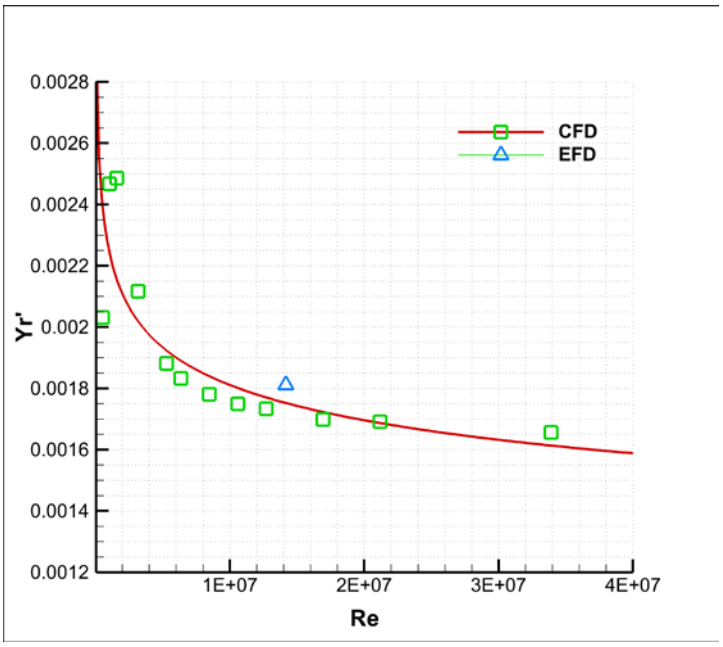

Figure 8. Re-Y_r' distribution of pure yaw.

Equation 14 and Equation 15 were obtained when the collected data as a result of CFD were fitted to the most appropriate equations. So, based on these two equations, if we have the Reynolds number of the bare hull form of the DARPA, we can calculate the Y_r' and N_r'.

$$Y_r' = -0.0001890118 \ln(\mathrm{Re}) + 0.004868874 \quad (14)$$

$$N_r' = 0.0001419491 \ln(\mathrm{Re}) - 0.003349958 \quad (15)$$

The length between perpendicular of DARPA L_{pp} = 4.261 m and the service speed of DARPA U_0 = 3.34 m/s in the experiment so the Reynolds number can be calculated as Re = $1.42*10^7$. Linear hydrodynamic coefficients can be obtained by placing this Reynolds number in equations 12, 13, 14, and 15, respectively. The comparison of the coefficients determined as a result of CFD and the experimental results published by DTRC (Roddy, 1990) are shown in Table 12.

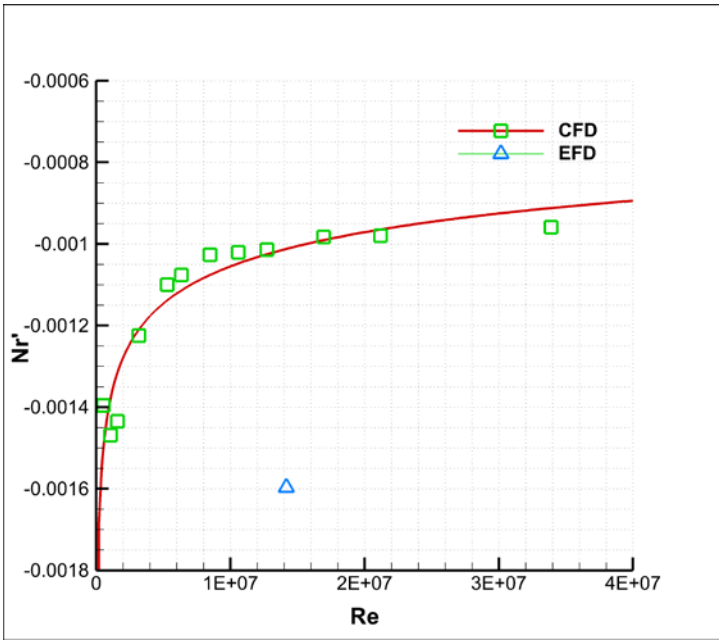

Figure 9. Re-N_r' distribution of pure yaw.

Table 12. Comparison of CFD and EFD results.

	Y_v'	N_v'	Y_r'	N_r'
EFD	-0.005948	-0.012795	0.001811	-0.001597
CFD	-0.006398	-0.013697	0.001756	-0.001013
Error	7.6%	7.1%	3.0%	36.6%

6. CONCLUSION

Maneuverability is one of the major design parameters especially for underwater vehicles to ensure proper handling and safety of the vessel. With recent advances in CFD capabilities and computational power, researchers have taken great interest in investigating issues with maneuverability using CFD. In this paper, the bare hull form of the DARPA geometry named AFF-1 configuration, which has plenty of previous results in the literature, has been studied. The study investigates the effects of scale on maneuver derivatives using various Reynolds numbers. By scaling the length and speed of this form, static drift and pure yaw simulations at 12 different Reynolds numbers were conducted with the help of CFD. From these simulations, linear hydrodynamic coefficients were calculated and used to establish logarithmic relationships between Reynolds number and maneuvering derivatives. Finally, the CFD-generated coefficients are compared to previously published experimental results.

Although the results in the Y_v', N_v', and Y_r' maneuvering derivatives are very close to the experimental results, there is a difference between the CFD and the test result in N_r'. It is known that N_r' is very sensitive to center of gravity of the vessel; any small change in this value might reflect as a big difference in this hydrodynamic coefficient. Despite this discrepancy, our study reveals the dependency of the hydrodynamic coefficients on the Reynolds number. Speed variation tests in some mathematical models try to compensate this deficiency of the state-of-the-art, but it is believed that the utilization of hydrodynamic coefficients as a function of the Reynolds number will increase the accuracy of maneuvering simulations.

APPENDIX

Abbreviation

CFD	:	Computational Fluid Dynamics
EFD	:	Experimental Fluid Dynamics
DOF	:	Degrees of Freedom
DTRC	:	David Taylor Research Center
FVM	:	Finite Volume Method
LCB	:	Longitudinal Center of Buoyancy
RANS	:	Reynolds Averaged Navier Stokes

Nomenclature

D	:	Diameter of Submarine
Fr	:	Froude Number
I_Z	:	Moment of Inertia of Yaw
L_{OA}	:	Length Overall of Submarine
L_{PP}	:	Length Between Perpendicular of Submarine
m	:	Mass of Submarine
m_x	:	Added Mass of x Axis Direction
N	:	Yaw Moment
N_H	:	Yaw Moment on the Hull Around The z Axis
N_r	:	1st Order Derivative Coeff. of N Moment Respect to r
N_r'	:	Non-Dimensionalized N_r
N_{rrr}	:	3rd Order Derivative Coeff. of N Moment Respect to r
N_v	:	1st Order Derivative Coeff. of N Moment Respect to v
N_v'	:	Non-Dimensionalized N_v
N_{vvv}	:	3rd Order Derivative Coeff. of N Moment Respect to v
$N_{\dot{v}}$	:	Added Mass Coefficient of N Moment Respect to $\dot{v}$
$N_{\dot{r}}$	:	Added Mass Coefficient of N Moment Respect to $\dot{r}$
r	:	Yaw Angular Velocity of Submarine
$\dot{r}$	:	Yaw Angular Acceleration of Submarine
Re	:	Reynolds Number
u	:	Longitudinal Velocity of Submarine
U_0	:	Service Speed of Submarine
v	:	Lateral Velocity of Submarine
X	:	Surge Force

x_G	:	Longitudinal Center of Gravity
$\ddot{x}_G$	:	Acceleration at x Axis
X_H	:	Surge Force on the Hull in The x Axis
Y	:	Sway Force
Y_H	:	Sway Force on the Hull in The y Axis
Y_r	:	1st Order Derivative Coeff. of Y Force Respect to r
Y_r'	:	Non-Dimensionalized Y_r
Y_{rrr}	:	3rd Order Derivative Coeff. of Y Force Respect to r
Y_v	:	1st Order Derivative Coeff. of Y Force Respect to v
Y_v'	:	Non-Dimensionalized Y_v
Y_{vvv}	:	3rd Order Derivative Coeff. of Y Force Respect to v
$\ddot{y}_G$	:	Acceleration at y Axis
$Y_{\dot{v}}$	:	Added Mass Coefficient of Y Force Respect to $\dot{v}$
$Y_{\dot{r}}$	:	Added Mass Coefficient of Y Force Respect to $\dot{r}$
ρ	:	Water Density

CONFLICT OF INTEREST STATEMENT

The authors declare no conflict of interest.

REFERENCES

Budak, G., & Beji, S. (2016). "Computational resistance analyses of a generic submarine hull form and its geometric variants." *The Journal of Ocean Technology , 76-86.*

Can, M. (2014). *Numerical simulation of hydrodynamic planar motion mechanism test for underwater vehicles.* [M.Sc. Thesis]. Middle East Technical University.

Çavdar, F. & Bal, Ş. (2022). "An investigation of hydrodynamic maneuvering derivatives and horizontal stability of DARPA suboff depending on depth." *Gemi ve Deniz Teknolojisi , (221) , 42-58 . 10.54926/gdt.1084413*

Feldman, J. (1979). "DTNSRDC revised standard submarine equations of motion."

He, S., Kellett, P., Yuan, Z., Incecik, A., Turan, O., & Boulougouris, E. (2016). "Manoeuvring prediction based on CFD generated derivatives." *Journal of Hydrodynamics, 28, 284-292.*

Kahramanoglu, E. (2023). "Numerical investigation of the scale effect on the horizontal maneuvering derivatives of an underwater vehicle." https://ssrn.com/abstract=4280314

Kırıkbaş, O., Kınacı, Ö. K. & Bal, Ş. (2021). "Sualtı araçlarının manevra karakteristiklerinin değerlendirilmesi-I: manevra analizlerinde kullanılan yaklaşımlar." *Gemi ve Deniz Teknolojisi , (219) , 6-58.*

Krishnakumar & Ramasamy, S., & Al-Mamun, A. (2018). "A study on dynamic positioning system robustness with wave loads predictions from deep belief network." 1520-1527. 10.1109/SSCI.2018.8628825.

Racine, B., & Paterson, E. (2005). "CFD-based method for simulation of marine-vehicle maneuvering." 10.2514/6.2005-4904.

Ray, A., & Singh, S., & Seshadri, V. (2009). "Evaluation of linear and nonlinear hydrodynamic coefficients of underwater vehicles using CFD." 10.1115/OMAE2009-79374.

Roddy, R.F. (1990). “Investigation of the stability and control characteristics of several configurations of the DARPA suboff model (DTRC Model 5470) from captive-model experiments.”

Shenoi, R., & Krishnankutty, P. & Selvam, Panneer. (2013). “Prediction of maneuvering coefficients of a container ship by numerically simulating HPMM using RANSE based solver.”

Sukas, O. F., Kinaci, Ö. K., & Bal, Ş. (2019). “System-based prediction of maneuvering performance of twin-propeller and twin-rudder ship using a modular mathematical model.” *Applied Ocean Research , vol.84, 145-162.*

Sukas, Ö. F., Kınacı, Ö. K., & Bal, Ş. (2017). “Gemilerin manevra performans tahminleri için genel bir değerlendirme 1.” *Gemi ve Deniz Teknolojisi , vol.23, no.210, 37-75.*

Triantafyllou S., & Hover S. (2003). *Manoeuvring and control of marine vehicles*, Department of Ocean Engineering, Massachusetts Institute of Technology, Cambridge, Massachusetts USA.

Vaz, G., & Toxopeus, S., & Holmes, S. (2010). “Calculation of manoeuvring forces on submarines using two viscous-flow solvers.” *Proceedings of the international conference on offshore mechanics and arctic engineering* - OMAE. 6. 10.1115/OMAE2010-20373.

Wang, H., & Zhai, Z. (2012). “Analyzing grid independency and numerical viscosity of computational fluid dynamics for indoor environment applications.” *Building and Environment. 52.* 107-118. 10.1016/j.buildenv.2011.12.019.

Yasukawa, H., & Yoshimura, Y. (2015). “Introduction of MMG standard method for ship maneuvering predictions.” *Journal of Marine Science and Technology, 20, 37-52.*

Yoon, H. (2009). “Phase-averaged stereo-PIV flow field and force/moment/motion measurements for surface combatant in PMM maneuvers.” [PhD Dissertation]. The University of Iowa.